ACS Medicinal Chemistry Letters

Letter

pubs.acs.org/acsmedchemlett

Discovery of RAF265: A Potent mut-B-RAF Inhibitor for the Treatment of Metastatic Melanoma

Teresa E. Williams, Sharadha Subramanian, Joelle Verhagen, Christopher M. McBride, Abran Costales, Leonard Sung, William Antonios-McCrea, Maureen McKenna, Alicia K. Louie, Savithri Ramurthy, Barry Levine, Cynthia M. Shafer, Timothy Machajewski, Paul A. Renhowe, Brent A. Appleton, Payman Amiri, James Chou, Darrin Stuart, Kimberly Aardalen, and Daniel Poon*

Global Discovery Chemistry, Oncology and Exploratory Chemistry, Novartis Institutes for Biomedical Research, 5300 Chiron Way, Emeryville, California 94608, United States

Supporting Information

ABSTRACT: Abrogation of errant signaling along the MAPK pathway through the inhibition of B-RAF kinase is a validated approach for the treatment of pathway-dependent cancers. We report the development of imidazo-benzimidazoles as potent B-RAF inhibitors. Robust *in vivo* efficacy coupled with correlating pharmacokinetic/pharmacodynamic (PKPD) and PD-efficacy relationships led to the identification of RAF265, **1**, which has advanced into clinical trials.

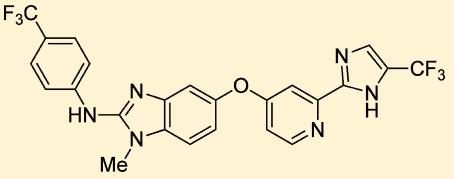

KEYWORDS: *B-RAF, MAP, VEGF, serine/threonine kinases, tyrosine kinases*

The MAPK signaling pathway, consisting of RAS/RAF/MEK/ERK, transduces input from cell surface receptors to nuclear transcription factors thereby regulating cellular proliferation, differentiation, and survival.[1] Dysregulation of this pathway through an activating mutation in B-RAF (V600E) occurs in ∼50% of melanomas and has made RAF the subject of many drug discovery efforts.[2] Validation for targeting B-RAF^{V600E} as an effective chemotherapeutic approach has been provided by the recent approval of vemurafenib (Roche) and dabrafenib (GSK) by the FDA for the treatment of metastatic melanoma (Figure 1).[3−5]

Previous publications from our laboratories have described the development of the 2-arylaminobenzimidazole scaffold as a platform for improved mut-RAF potency and pharmacokinetics over sorafenib (Bayer, Figure 1), an earlier receptor tyrosine kinase inhibitor approved for the treatment of renal cell and hepatocellular carcinoma.[6−8] In this report, we describe our continued efforts in this area, which resulted in the discovery of RAF265 (**1**), a potent inhibitor of B-RAF^{V600E} with complementary VEGFR and PDGFR activity.

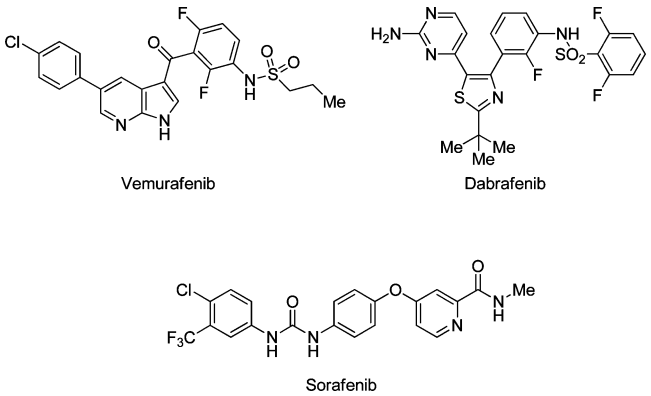

Figure 1. Structures of vemurafenib, dabrafenib, and sorafenib.

As reported previously, amido-2-arylaminobenzimidazoles, such as **2** (Table 1), have demonstrated potent biochemical inhibition as well as cellular activity in target modulation and proliferation assays against SKMEL-28, a B-RAF^{V600E} harboring melanoma cell line.[5−7,9]

Further development of the series did not result in further improvement in cellular potency; however, a simple and

Table 1. Key Amide Transformations[a]

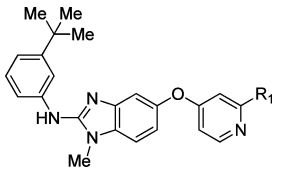

Cpd	R_1	B-RAF^{V600E}[b]	pERK SKMEL-28[c]	SKMEL-28[d]
2	−CONHMe	0.045 (1)	0.28 (3)	0.90 (3)
3	−NHCOMe	0.003 (1)	0.044 (7)	0.18 (8)
4	2-imidazolyl	0.090 (1)	0.39 (1)	

[a]IC_{50} in μM. Numbers in parentheses represent number of determinations. [b]B-RAF^{V600E} enzymatic assay.[6,7] Assay variability within 2-fold of the mean value of the control. [c]pERK SKMEL target modulation.[5,9] Assay variability within 3-fold of mean value for applicable entries. [d]SKMEL-28 cell proliferation assay.[5,9] Assay variability within 3-fold of mean value.

Received: December 19, 2014
Accepted: July 20, 2015
Published: August 3, 2015

DOI: 10.1021/ml500526p
ACS Med. Chem. Lett. 2015, 6, 961−965

effective inversion of the amide connectivity as embodied in **3** realized a marked increase in cellular potency.[7] Unfortunately, some substituted reverse amide analogues suffered from plasma instability, and an alternative moiety was sought. Utilizing an isostere replacement approach, cyclization of the forward amide of **2** led to the simple imidazole analogue **4**, which demonstrated a similar *in vitro* potency profile and provided a suitable starting point for further investigation.

The general synthetic route for the imidazole series is represented by the synthesis of **1** as depicted in Scheme 1. The

Scheme 1. Synthesis of 1[a]

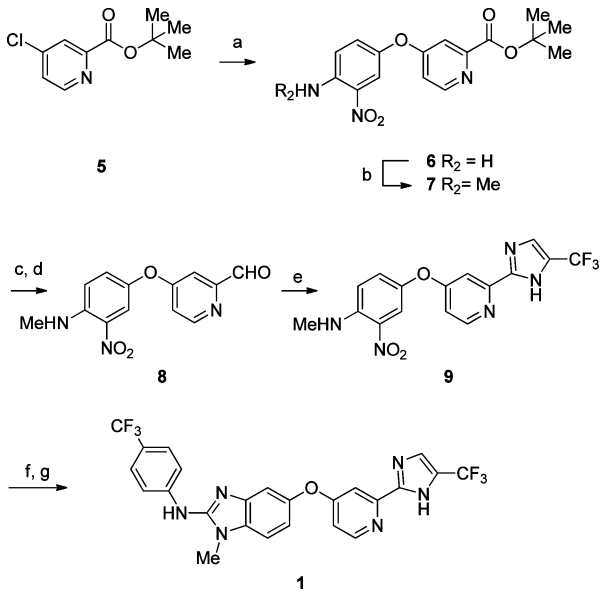

[a]Reagents and conditions: (a) 3-nitro-4-aminophenol, K_2CO_3, DMSO, 100 °C, 74%; (b) TFAA, DCM, 0 °C; Me_2SO_4, TBACl, 10% NaOH, 76%; (c) LAH, THF 0 °C; $NaBH_4$, 46%; (d) MnO_2, DCM, 58%; (e) 1,1-dibromo-3,3,3-trifluoroacetone, NaOAc, water, 100 °C; NH_4OH, MeOH rt, 91%; (f) 10% Pd/C, H_2, MeOH/EtOAc, 96%; (g) 4-trifluoromethylphenyl thioisocyanate, $FeCl_3$, 40−60%.

central phenyl-pyridyl ether **6** was assembled from the S_NAr reaction of chloropyridine **5** with 3-nitro-4-aminophenol. Methylation of the anilino nitrogen was accomplished using phase transfer catalysis to give **7**.[10,11] Reduction of the *t*-butyl ester using LAH under strict temperature control, followed by $NaBH_4$ and MnO_2 oxidation furnished aldehyde **8**. Debus−Radziszewski cyclization with an *in situ* generated glyoxal derived from 1,1-dibromo-3,3,3-trifluoroacetone furnished the corresponding imidazole **9**.[12] Reduction of the nitroarene followed by addition of 4-trifluoromethylphenyl thioisocyanate and $FeCl_3$-promoted ring cyclization provided **1**.[13] All compounds where biological data is presented have >95% purity as determined by HPLC.

The simple, unadorned imidazole **4**, while providing a useful benchmark against the previous series, did not offer the cellular potency desired and resulted in a significant CYP liability (CYP3A4 IC_{50} = 1.8 μM). An SAR campaign probing the anilide and imidazole substitution patterns was undertaken to address cellular potency and CYP3A4 inhibition of this series (Table 2).

Holding with previously reported SAR trends, 3- and 4-position branched alkyl substituents of the anilide ring conferred potency (**4**, **10**−**12**).[4,5] For meta-substituted

Table 2. Selected Data from Anilide and Imidazole SAR Survey[a]

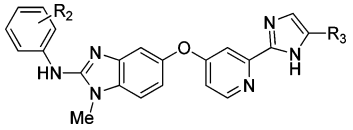

Cpd	R_2	R_3	pERK SKMEL-28[b]	SKMEL-28[c]	CYP3A4[d]
4	3-*t*Bu	H	0.39 (1)		1.8 (2)
10	3-*t*Bu	Ph	0.48 (2)	1.1 (1)	7.1 (1)
11	3-*t*Bu	CF_3	0.12 (2)	0.12 (2)	10 (3)
12	4-*t*Bu	CF_3	0.13 (1)	0.23 (1)	34 (1)
13	2-F, 5-*t*Bu	CF_3	0.042 (1)	0.050 (1)	3.3 (1)
14	3-CF_3	CF_3	0.78 (1)	1.62 (1)	>40 (1)
15	2-F, 5-CF_3	CF_3	0.21 (4)	0.6 (4)	26 (2)
16	2-F, 5-CF_3	Me	0.62 (1)	0.74 (1)	3.4 (1)
1	4-CF_3	CF_3	0.14 (18)	0.16 (12)	>40 (3)

[a]IC_{50} in μM. Numbers in parentheses represent number of determinations. [b]pERK SKMEL target modulation.[7,8] [c]SKMEL28 cell proliferation assay.[7,8] [d]CYP3A4 inhbition assay using midazolam as subtrate. Assay variability within 2-fold of mean value for applicable entries. See Supporting Information for CYP3A4 assay conditions and isoform inhibition of **1**.

analogues, introduction of a fluorine at the 2-position gave a further boost in cellular potency (**13**, **15**). Unfortunately, all 3- and 5-alkyl substituted analogues suffered from poor exposure in pharmacokinetic (PK) studies. A solution was found in the *para*- and *meta*-CF_3 analogues (**1**, **14**), which provided a similar level of potency as with the alkyl analogues along with greater metabolic stability. In examining the imidazole substitution pattern, it was observed that electron withdrawing groups improved cellular potency as illustrated in the matched pair analyses of **4**, **11** and **15**, **16**. Gratifyingly, imidazole substitution also provided incremental reduction in CYP3A4 inhibition[14] (**4**, **10**, **11**); however, the CYP3A4 profile could be further modulated by the anilide substitution pattern. Moving the *t*Bu group from the 3-position to the 4-position (**12**) resulted in an improvement in CYP3A4 selectivity, which also translated into the corresponding CF_3 analogue **1**. With a favorable balance of cellular potency and CYP3A4 selectivity, **1** was selected for further investigation.

The crystal structure of **1** in truncated wt-B-RAF provided insight as to how the molecule interacts with the target protein (Figure 2).[15] Binding occurred through a Type II, inactive-like conformation where the DFG loop has adopted an "out"

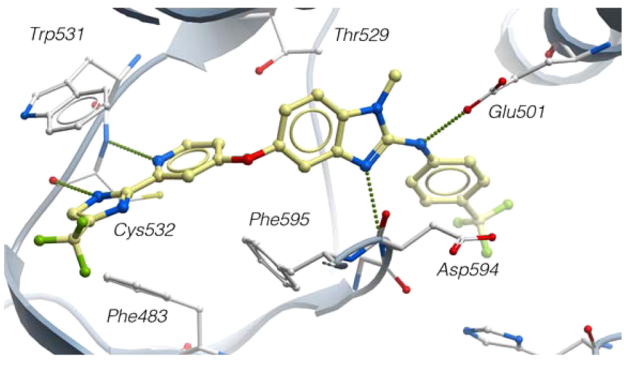

Figure 2. Co-crystal structure of **1** bound to truncated wt-B-RAF at 3.2 Å resolution.

DOI: 10.1021/ml500526p
ACS Med. Chem. Lett. 2015, 6, 961−965

Table 3. Biochemical Activities Against Select Tyrosine Kinases[a]

Cpd	B-RAF^{V600E}	VEGFR	c-KIT	PDGFRβ	LCK	FYN	SRC
2	0.045	0.005	0.010	0.010	0.065	0.005	
3	0.003	0.002	0.003	0.001	0.003	0.002	0.002
4	0.090	0.030	0.020	0.31	0.20	0.040	
11	0.055	0.070	0.020	0.001	2.0	0.22	>6.0
1	0.020	0.020	0.020	0.006	>6.0	>10	>10

[a]IC_{50} in μM. All entries are single determinations. See ref 19 for a broader kinase survey of **1**.

conformation.[16] Of interest is the hinge region where the imidazole is situated between Trp531 and Phe483. The imidazole NH interacts with the carbonyl of Cys532, suggesting that a potential role of the 5-CF_3 substituent is to acidify the NH-bond and facilitate a stronger hydrogen bonding interaction. The pyridyl moiety makes a second hydrogen bond to Cys532 that completes an efficient bidentate interaction. The ring benzimidazolo nitrogen and the anilide NH are found to hydrogen bond with the NH backbone of Asp594 of the DFG loop and Glu501 of the αC-helix, respectively.[17] The NMe of the benzimidazole fills the selectivity pocket partially defined by the "gatekeeper" residue, Thr529.

RAF265 (**1**) was found to be a potent inhibitor of B-RAF^{V600E}, wt-B-RAF, and C-RAF with IC_{50}s of 0.0005, 0.070, and 0.019 μM, respectively. The kinase selectivity profile of **1** bore similarities to inhibitors of other serine/threonine and tyrosine kinases, such as sorafenib.[16−19] All specific hydrogen bonds between **1** and wt-B-RAF are with residues that are conserved among the kinases (e.g Glu501 and Asp594). Within the chemical series, consistent off targets included VEGFR, PDGFβ, and c-Kit, all of which share a threonine or a similarly sized valine residue at the gatekeeper position in the "back" or "selectivity" pocket (Table 3).

Kinase profiling of each of the benzimidazolo archetypes (**2**, **3**, **4**) indicated little or no discrimination against a significant segment of tyrosine kinases. However, within the imidazole series, substitution at imidazole in the hinge region provided a handle to address selectivity against the SRC family of kinases (**11**, **1**). To understand the selectivity profile in a cellular setting, **1** was evaluated in a panel of Ba/F3 cells whose profileration was dependent on a range of protein kinases (Figure 3).[20]

The activity against these kinase-dependent cell lines (KDR, KIT, PDGFRb) recapitulated the biochemical findings and were corroborated by a cell based receptor phosphorylation assay (VEGFR IC_{50} = 0.19 μM). This level of activity was similar to that observed against Ba/F3-B-RAF^{V600E} (IC_{50} = 0.14 μM) and in the SKMEL-28 proliferation assay. Conversely, the Ba/F3 cells expressing LCK, FYN, and SRC were not inhibited reflecting success in achieving selectivity against these kinases. Together, these data indicated that along with potent inhibition of B-RAF^{V600E}, **1** also inhibited the VEGFR and PDGFR family of kinases, which play critical roles in tumor angiogenesis.

Pathway inhibition and antiproliferative effects were evaluated in a small panel of tumor cell lines (Figure 4).

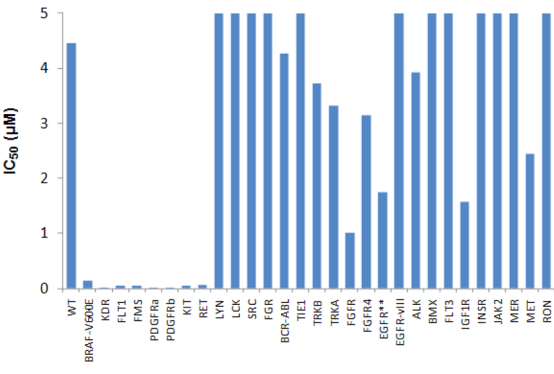

Figure 3. Inhibitory activity of **1** against kinase dependent Ba/F3 cell lines. IC_{50} in μM. All entries are single determinations.

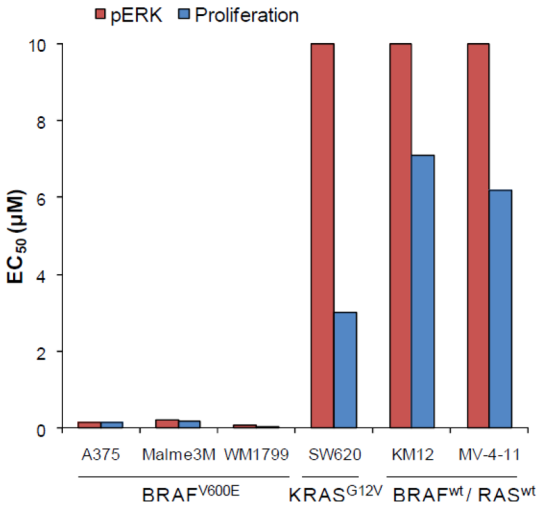

Figure 4. *In vitro* target modulation and antiproliferation of RAF265 on MAPK-dependent tumor cell lines. IC_{50} in μM. All entries are single determinations. See Supporting Information for assay details.

In melanoma tumor cell lines expressing B-RAF^{V600E} (A375, Malme-3M, and WM-1799), **1** decreased phospho-ERK and inhibited proliferation with IC_{50} ranging from 0.04 to 0.2 μM. In contrast, cell lines that expressed wt-B-RAF, **1**, failed to suppress phospho-ERK levels and had weak antiproliferative activity.

Owing to the size and lipophilic nature of the molecule (MW = 518, cLog P > 5), it was unsurprising that **1** exhibited poor kinetic aqueous solubility (~1 μM) and high plasma protein binding (>99% PPB in mouse, rat, dog, and human).[21] Despite these drawbacks, **1** exhibited good to moderate oral bioavailability across species, with dog being the lowest, when dosed in single dose PK studies (Table 4). Total plasma clearance is very low relative to hepatic blood flow, and the plasma half-life across species is greater than 24 h, indicating the possibility of accumulation in multidose settings.

In mouse PK studies, the high plasma protein binding and a low volume of distribution of **1** would suggest sequestration within the plasma compartment. In separate efficacy studies in A375M xenograft models, **1** was able to distribute to the target

DOI: 10.1021/ml500526p
ACS Med. Chem. Lett. 2015, 6, 961−965

Table 4. *In Vivo* Pharmacokinetics of 1 Across Species[a]

parameters	mouse	rat	dog	monkey
dose (mpk, iv/po)	5, 30	5, 20	1.25, 5	1, 5
%*F*	51	>95	35	48
$AUC_{\infty, po}$ (μM·h)	4300	450	35	48
CL (mL/min/kg)	0.1	0.9	0.8	1.5
Vss (L/kg)	0.5	3.3	1.9	2.9
$t_{1/2}$ (h)	41	46	27	28

[a]Administered as a solution in 60%PEG400/40% PG.

and exert a pronounced pharmacological effect (Figures 5 and 6).

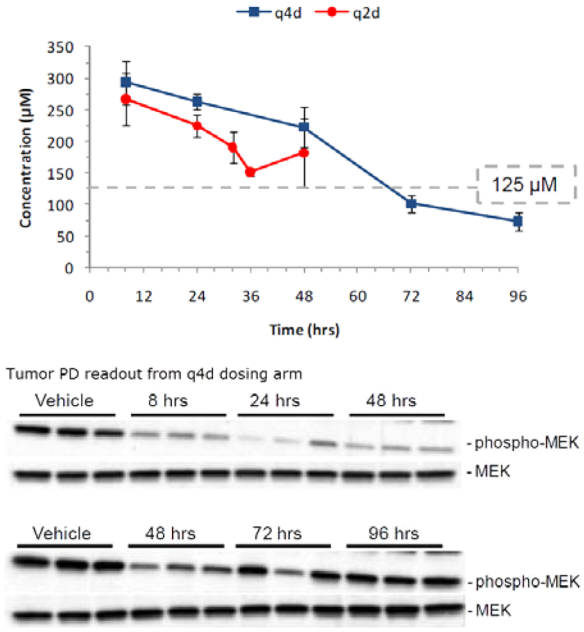

Figure 5. PKPD snapshot from A375M model xenograft model. PD sampling taken at noted time points post-third dose of the q4d arm. The PD readouts of the 48 h time point are two separate blots of the same tumor lysate sample. See Supporting Information for efficacy data and experimental details.

Seeking to take advantage of the long PK half-life, a 32 day multidose efficacy study examining the effect of intermittent dosing regimens on target coverage was undertaken. Tumors from a subset of mice from each study arm were harvested at intervals post-third dose, and the corresponding lysates were assayed for phospho-MEK levels by Western blot analysis (Figure 5). Dosing q2d maintained a C_{min} trough level of ~125 μM, which corrected for mouse plasma protein (99.6%) yielding an effective free C_{min} of ~0.5 μM (A375M IC_{50} = 0.16 μM). The pharmacodynamic (PD) readout from the q4d arm indicated significant target suppression out to 48 h followed by complete signal recovery at 96 h, indicating that the q2d dosing regimen would be optimal for target coverage.

To characterize the dose−response relationship, **1** was dosed orally q2d at 10, 30, and 100 mg/kg in a 28 day mouse efficacy study (Figure 6). Consistent with the results of the previous study in Figure 5, **1** induced tumor regressions at the 100 mg/kg, while at 30 mg/kg resulted in robust stasis or tumor growth inhibition, and the 10 mg/kg dose demonstrated modest inhibition of tumor growth relative to vehicle treated animals. The PD results corroborated the earlier PKPD findings with

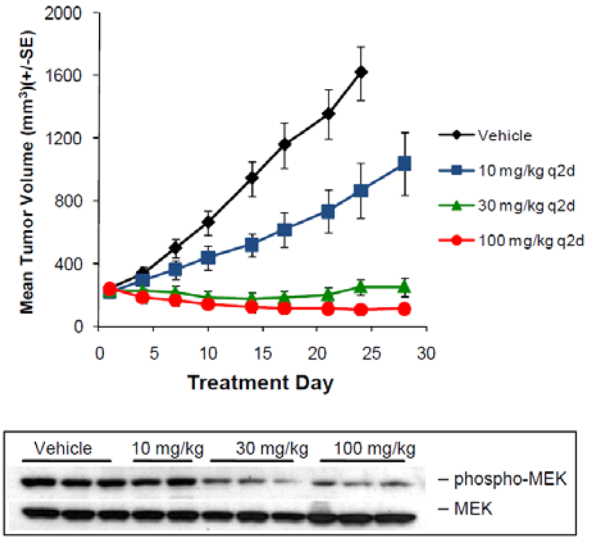

Figure 6. Efficacy of **1** in A375M mouse xenograft. PD sampling taken 4 h post-third dose. Less than 15% body weight loss was observed in the 100 mg/kg q2d dosing arm. See Supporting Information for more details.

the 30 and 100 mg/kg dose, which resulted in significant reductions in phospho-MEK levels compared to tumors from the vehicle group, while the 10 mg/kg dose did not appreciably alter phospho-MEK levels.

To conclude, we have developed a novel chemical series derived from 2-arylaminobenzimidazoles, which were optimized for cellular potency while balancing kinase selectivity and ADME properties. These efforts resulted in the identification of **1** as a potent inhibitor of B-RAF^{V600E} with complementary VEGFR and PDGFR activity that demonstrated potent *in vivo* target modulation and efficacy. Further development of this molecule resulted in the advancement into clinical trials for the treatment of metastatic melanoma.[22]

■ ASSOCIATED CONTENT

Supporting Information

Experimental details for the synthesis and characterization of select compounds, procedures for the biochemical and cellular assays, *in vivo* analyses, and crystallographic conditions. The Supporting Information is available free of charge on the ACS Publications website at DOI: 10.1021/ml500526p.

■ AUTHOR INFORMATION

Corresponding Author

*E-mail: daniel.poon@novartis.com.

Notes

The authors declare no competing financial interest.

■ ACKNOWLEDGMENTS

The authors wish to acknowledge Mina Aikawa and Susan Fong for their support on cellular and biochemical assays, Ahmad Hashash on formulations, Jeremy Murray on preliminary structural work, and Oncotest GmBH (Breisgrau, Germany) for providing support on xenograft PKPD models.

■ REFERENCES

(1) Santarpia, L.; Lippman, S. M.; El- Naggar, A. K. Targeting the MAPK-RAS-RAF signaling pathway in cancer therapy. *Expert Opin. Ther. Targets* **2012**, *16*, 103−119.

DOI: 10.1021/ml500526p
ACS Med. Chem. Lett. 2015, 6, 961−965

(2) Davies, H.; Bignell, G. R.; Cox, C.; Stephens, P.; Edkins, S.; Clegg, S.; Teague, J.; Woffendin, H.; Garnett, M. J.; Bottomley, W.; Davis, N.; Dicks, E.; Ewing, R.; Floyd, Y.; Gray, K.; Shall, S.; Hawes, R.; Hughes, J.; Kosmidou, V.; Menzies, A.; Mould, C.; Parker, A.; Stevens, C.; Watt, S.; Hooper, S.; Wilson, R.; Jayatilake, H.; Gusterson, B. A.; Cooper, C.; Shipley, J.; Hargrave, D.; Pritchard-Jones, K.; Maitland, N.; Chenevix-Trench, G.; Riggins, G. J.; Bigner, D. D.; Palmieri, G.; Cossu, A.; Flanagan, A.; Nicholson, A.; Ho, J. W. C.; Leueng, S. Y.; Yuen, S. T.; Weber, B. L.; Seigler, H. F.; Darrow, T. L.; Paterson, H.; Marais, R.; Marshall, C. J.; Wooster, R.; Stratton, M. R.; Futreal, P. A. Mutations of the *B-RAF* gene in human cancer. *Nature* **2002**, *417*, 949−954.

(3) Martin-Liberal, J.; Larkin, J. New RAF kinase inhibitors in cancer therapy. *Expert Opin. Pharmacother.* **2014**, *15*, 1235−1245.

(4) Bollag, G.; Tsai, J.; Zhang, J.; Zhang, C.; Ibrahim, P.; Nolop, K.; Hirth, P. Vemurafenib: the first drug approved for BRAF-mutant cancer. *Nat. Rev. Drug Discovery* **2012**, *11*, 873−886.

(5) Rheault, T. R.; Stellwagen, J. C.; Adjabeng, G. M.; Hornberger, K. R.; Petrov, K. G.; Waterson, A. G.; Dickerson, S. H.; Mook, R. A.; Laquerre, S. G.; King, A. J.; Rossanese, O. W.; Arnone, M. R.; Smitheman, K. N.; Kane-Carson, L. S.; Han, C.; Moorthy, G. S.; Moss, K. G.; Uehling, D. E. Discovery of Dabrafenib: A selective inhibitor of Raf kinases with antitumor activity against B-Raf driven tumors. *ACS Med. Chem. Lett.* **2013**, *4*, 358−362.

(6) Ramurthy, S.; Subramanian, S.; Aikawa, M.; Amiri, P.; Costales, A.; Dove, J.; Fong, S.; Jansen, J. M.; Levine, B.; Ma, S.; McBride, C. M.; Michaelian, J.; Pick, T.; Poon, D. J.; Girish, S.; Shafer, C. M.; Stuart, D.; Sung, L.; Renhowe, P. A. Design and Synthesis of Orally Bioavailable Benzimidazoles as RAF kinasse inhibitors. *J. Med. Chem.* **2008**, *51*, 7049−7052.

(7) Subramanian, S.; Costales, A.; Williams, T.; Levine, B.; McBride, C.; Poon, D.; Amiri, P.; Renhowe, P.; Shafer, C.; Stuart, D.; Verhagen, J.; Ramurthy, S. Design and synthesis of orally bioavailable benzimidazole reverse amides as pan-RAF kinase inhibitors. *ACS Med. Chem. Lett.* **2014**, *5*, 989−992.

(8) Wilhelm, S.; Carter, C.; Lynch, M.; Lowinger, T.; Dumas, J.; Smith, R. A.; Schwartz, B.; Simantov, R.; Kelley, S. Discovery and development of sorafenib: a multikinase inhibitor for treating cancer. *Nat. Rev. Drug Discovery* **2006**, *5*, 835−844.

(9) Tsai, J.; Lee, J. T.; Wang, W.; Zhang, J.; Cho, H.; Mamo, S.; Bremer, R.; Gillette, S.; Kong, J.; Haass, N. K.; Sproesser, K.; Li, L.; Smalley, K. S. M.; Fong, D.; Zhu, Y. L.; Marimuthu, A.; Nguyen, H.; Lam, B.; Liu, J.; Cheung, I.; Rice, J.; Suzuki, Y.; Luu, C.; Settachatgul, C.; Shellooe, R.; Cantwell, J.; Kim, S. H.; Schlessinger, J.; Zhange, K. Y. J.; West, B. L.; Powell, B.; Habets, G.; Zhang, C.; Ibrahim, P. N.; Hirth, P.; Artis, D. R.; Herlyn, M.; Bollag, G. Discovery of a selective inhibitor or oncogenic B-Raf kinase with potent antimelanoma activity. *Proc. Natl. Acad. Sci. U. S. A.* **2008**, *105*, 3041−3046.

(10) Brown, S. A.; Rizzo, C. J. A "one-pot" phase transfer alkylation/hydrolysis of *o*-nitrotrifluoroacetanilides. A convenient route to *N*-alkyl *0*-phenylenediamines. *Synth. Commun.* **1996**, *26*, 4065−4080.

(11) McKillop, A.; Fiaud, J. C.; Hug, R. P. The use of phase- transfer catalysis for the synthesis of phenol ethers. *Tetrahedron* **1974**, *30*, 1379−1382.

(12) Baldwin, J. J.; Kasinger, P. A.; Novello, F. C.; Sprague, J. M. 4-Trifluoromethylimidazoles and 5-(4-pyridyl)-1,2,4-triazoles, new classes of xanthine oxidase inhibitors. *J. Med. Chem.* **1975**, *18*, 895−900.

(13) An alternative process procedure has been described: Artman, G.; Solovay, C. F.; Adams, C. M.; Diaz, B.; Dimitroff, M.; Ehara, T.; Gu, D.; Ma, F.; Liu, D.; Miller, B. R.; Pick, T. E.; Poon, D. J.; Ryckman, D.; Siesel, D. A.; Stillwell, B. S.; Swiftney, T.; van Dyck, J. P.; Zhang, C.; Ji, N. One pot synthesis of aminobenzimidazoles using 2-chloro-1,2-dimethylimidazolium chloride (DMC). *Tetrahedron Lett.* **2010**, *51*, 5319−5321.

(14) Tyagarajan, S.; Chakravarty, P. K.; Zhou, B.; Fisher, M. H.; Wyvratt, M. J.; Lyons, K.; Klatt, T.; Li, X.; Kumar, S.; Williams, B.; Felix, J.; Priest, B. T.; Brochu, R. M.; Warren, V.; Smith, M.; Garcia, M.; Kaczorowski, G. J.; Martin, W. J.; Abbadie, C.; McGowan, E.; Jochnowitz, N.; Parsons, W. H. Substitutied biaryl oxazoles, imidazoles, and thiazoles as sodium channel blockers. *Bioorg. Med. Chem. Lett.* **2010**, *20*, 5536−5540.

(15) Coordinates and structure factors have been deposited in the Protein Data Bank (www.rcsb.org) with the accession code 5ct7.

(16) Zhang, J.; Yang, P. L.; Gray, N. S. Targeting cancer with small molecule kinase inhibitors. *Nat. Rev. Cancer* **2009**, *9*, 28−39.

(17) Smith, A. L.; DeMorin, F. F.; Paras, N. A.; Huang, Q.; Petkus, J. K.; Doherty, E. M.; Nixey, T.; Kim, J. L.; Whittington, D. A.; Epstein, L. F.; Lee, M. R.; Rose, M. J.; Babij, C.; Fernando, M.; Hess, K.; Le, Q.; Beltran, P.; Carnahan, J. Selective inhibitors of the mutant-B-RAF Pathway: Discovery of a Potent and Orally Bioavailable Amino-isoquinoline. *J. Med. Chem.* **2009**, *52*, 6189−6192.

(18) Kumar, R.; Crouthamel, M. C.; Rominger, D. H.; Gontarek, R. R.; Tummino, P. J.; Levin, R. A.; King, A. G. Myelosupression and kinase selectivity of multikinase angiogenesis inhibitors. *Br. J. Cancer* **2009**, *101*, 1717−1723.

(19) A broad kinase survey was conducted on RAF265 and other kinase inhibitors: Karaman, M. W.; Herrgard, S.; Treiber, D. K.; Gallant, P.; Atteridge, C. E.; Campbell, B. T.; Chan, K. W.; Ciceri, P.; Davis, M. I.; Edeen, P. T.; Faraoni, R.; Floyd, M.; Hunt, J. P.; Lockhart, D. J.; Milanov, Z. V.; Morrison, M. J.; Pallares, G.; Patel, H. K.; Pritchard, S.; Wodicka, L. M.; Zarrinkar, P. P. A quantitative analysis of kinase inhibitor selectivity. *Nat. Biotechnol.* **2008**, *26*, 127−132.

(20) Melnick, J. S.; Janes, J.; Kim, S.; Chang, J. Y.; Sipes, D. G.; Gunderson, D.; Jarnes, L.; Matzen, J. T.; Garcia, M. E.; Hood, T. L.; Beigi, R.; Cia, G.; Harig, R. A.; Asatryan, H.; Yan, S. F.; Zhou, Y.; Gu, X. J.; Saadat, A.; Zhou, V.; King, F. J.; Shaw, C. M.; Su, A. I.; Downs, R.; Gray, N. S.; Schultz, P. G.; Warmuth, M.; Caldwell, J. S. An efficient rapid system for profiling the cellular activities of molecular libraries. *Proc. Natl. Acad. Sci. U. S. A.* **2006**, *103*, 3153−3158.

(21) Arnott, J. A.; Planey, S. L. The influence of lipophilicity in drug discovery and design. *Expert Opin. Drug Discovery* **2012**, *7*, 863−875.

(22) Novartis Pharmaceuticals. A Study to Evaluate RAF265, an Oral Drug Administered to Subjects With Locally Advanced or Metastatic Melanoma. http://clinicaltrials.gov/show/NCT00304525 (NLM Identifier: NCT00304525).

DOI: 10.1021/ml500526p
ACS Med. Chem. Lett. 2015, 6, 961−965